

1
2
3
4
5
6
7
8
9
10
11
12
13
14
15
16
17

Effective Disinfection of *Escherichia coli* Contaminated Water Using Silver Nanoparticle-Decorated Magnetic Cobalt Cores

Jiin Yun¹ and Hyukmin Kweon^{2,3,*}

¹ Orange County School of the Arts, 1010 N Main St, Santa Ana, CA 92701, USA

² Civil and Environmental Engineering, University of California, Los Angeles, Los Angeles, California 90095, USA

³ BenSci Inc., 2321 W 10th Street, Los Angeles, CA 90006, USA

*Correspondence: kweonhyukmin@gmail.com

18 **Abstract**

19

20 In recent years, the development of silver nanoparticles (AgNPs) and their application in
21 wastewater treatment have emerged as highly effective disinfection methods. Wastewater
22 treatment processes effectively remove silver particles and colloids (most processes exceed 95%),
23 but this still leaves notable concentrations that escape to effluent-receiving waters. To address this
24 challenge, in this study, novel magnetic nanocomposites, silver nanoparticle-decorated magnetic
25 cobalt (AgNPs/Co), were studied for disinfection of water contaminated with Escherichia coli (E.
26 coli). First, the magnetic efficiency of the synthesized nanocomposites was measured. To measure
27 the disinfection efficiency of AgNPs/Co in E. coli-contaminated water, various studies have used
28 concentrations ranging from 10 to 50 µg. The results demonstrated an impressive antibacterial
29 efficiency rate of 99.6% when using AgNPs/Co. Additionally, the efficiency rate of collecting the
30 novel magnetic nanocomposites was found to be 100% using a magnet. The AgNPs/Co technology
31 not only exhibits highly efficient water purification capabilities, but also offers the added benefit
32 of complete removability using a magnet, a simple yet effective collection method. This feature
33 plays a crucial role in preventing the introduction of toxic AgNPs into reservoirs, which could
34 negatively impact both human populations and ecosystems. By enabling the production of clean
35 water while preserving the environment, this technology provides an innovative solution for
36 wastewater treatment.

37

38

39 **Keywords:** *Silver nanoparticles, Cobalt cores, Polyol method, Disinfection, Escherichia coli,*

40 *Wastewater*

41 1. INTRODUCTION

42 In the absence of adequate wastewater treatment, there is a persistent risk of diseases such
43 as cholera, typhoid, hepatitis A, and polio spreading[1]. Currently, chlorination, ultraviolet (UV)
44 radiation, and ozone are the most commonly used disinfection methods for US onsite wastewater
45 treatment systems. However, repeated use of chlorine has caused the evolution of chlorine-
46 resistant bacteria, which are not properly filtered out before the water is returned to the
47 environment.[2] UV radiation, which is effective against specific microorganisms, has a limited
48 scope. Additionally, ozone treatment fails to target the microorganisms' DNA and arginine, an
49 essential amino acid, which can facilitate horizontal gene transfer, thereby exacerbating public
50 health risks.[3] It is crucial to develop alternative and more efficient methods for wastewater
51 treatment to address these challenges and to ensure the protection of public health and the
52 environment.

53 Silver nanoparticles (AgNPs) are regarded as highly effective disinfectants for wastewater
54 treatment because of the antibacterial mechanisms of silver ions (**Figure 1**). The silver ions
55 released from nanoparticles disturb the permeability of the cell membrane upon attachment to the
56 bacterial wall.[4–6] After entering the cell, the ions 1) bind to sulfhydryl proteins, leading to
57 protein inactivation,[7] 2) interfere with the respiratory chain, causing oxidative stress,[8–10] and
58 3) disrupt DNA replication, resulting in lipid damage. Eventually, the bacterial wall and membrane
59 break as a result of cytoplasmic leakage, destroying the bacteria. AgNPs inactivate over 99% of
60 *Escherichia coli* (*E. coli*) bacteria after several seconds of contact.[11]

61

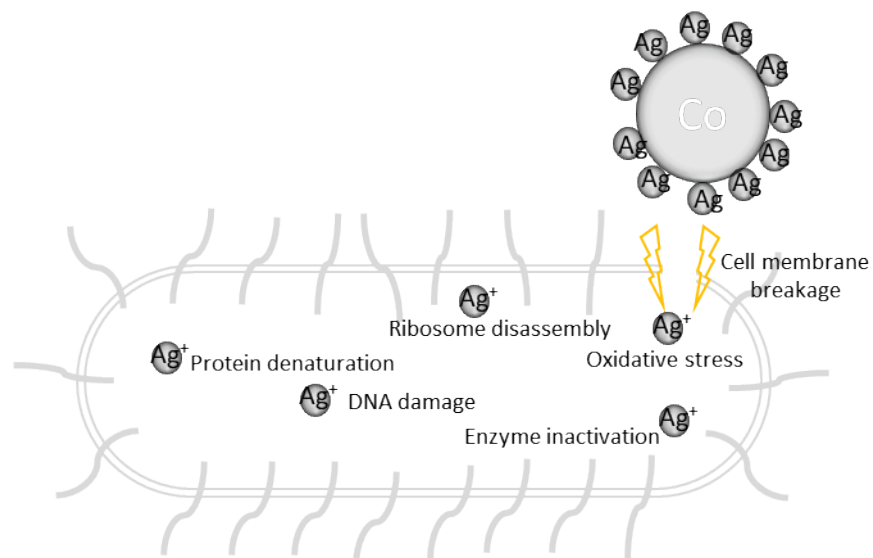


Figure 1. Mechanisms for antimicrobial actions of silver nanoparticle-decorated magnetic cobalt.

62

63 The widespread use of AgNPs in commercial and professional applications has resulted in
64 the regular ingestion of residual silver, estimated to be within the range of 20–80 micrograms (μg),
65 through sources such as water contamination, dietary supplements, and food packaging.[12,13] In
66 order to mitigate potential health risks associated with silver exposure, the Environmental
67 Protection Agency limits the daily exposure to silver to 5 μg per kilogram (kg) per day, which is
68 approximately 310 μg for the average human adult weighing 62 kg. AgNPs, upon binding to
69 various human tissues, can elicit toxic effects, including cell activation that leads to the generation
70 of reactive oxygen species, inflammation, and ultimately cell death.[12] Additionally, several
71 reports have documented instances of skin discoloration attributed to the toxicity of AgNPs.[14–
72 16] The absence of effective AgNPs collection not only poses a risk to human health, but also
73 impacts soil communities and aquatic systems.[17–21]

74 Although AgNPs have been proven to be an effective bactericide in water treatment
75 methods, the recollection of leached silver remains a challenge.[22] This research aimed to assess
76 the efficiency of using silver nanoparticles (AgNPs) in the bacterial removal of *E. coli* from a
77 contaminated water test solution and to explore the potential of using magnets to recollect AgNPs.
78 In this research, wastewater was defined by adding *E. coli* into the water matrix. In order to
79 recollect AgNPs using a magnet, silver nanoparticle-decorated magnetic cobalt (AgNPs/Co), was
80 synthesized by the polyol method, which is a widely-used cost-effective and facile soft chemical
81 nanoparticle synthesis method that has been proven to be scalable for industrial application and
82 effective in preparing core-shell nanostructures with tailored size and shapes.[23] In this study, a
83 modified polyol process with a transmetalation reduction method was adopted from Kanwal, et
84 al., (2019) and used to synthesize the desired silver nanoparticle coated cobalt core (Kanwal et al.,
85 2019).[24] This method allowed the fabrication of silver onto the cobalt core medium and control
86 of the nanoparticle size. In contrast to the referenced article, this research extended the boundaries
87 of exploration by evaluating the removal efficiency of nanoparticles through magnetic means. This
88 study also probed the potential implications of silver introduction into wastewater treatment plants,
89 specifically addressing concerns related to silver poisoning. By giving the nanoparticles a magnetic
90 property, the AgNPs/Co can be recollecting using magnets, a quick yet promising method of
91 preventing the silver from leaching into the environment.

92

93

94 **2. MATERIALS AND METHODS**

95 **2.1. Materials**

96 All chemicals, including cobalt acetate tetrahydrate, silver acetate, ethylene glycol,
97 polyvinylpyrrolidone (PVP), and hydrazinium hydroxide were purchased from Sigma Aldrich. As
98 reference, commercial silver nanoparticles (50,000 ppm in a 5 mL solution, diameter: 15nm) (US
99 Research Nanoparticles, US7160) were purchased. Nutrient agar (Innovating Science, IS5350)
100 purchased from Innovating Science was used for the antibacterial tests. *E. coli* (Carolina Biological,
101 #155065) was purchased from Carolina Biological. An incubator (VEVOR, XHC-25) was
102 purchased from Vevor to let the *E. coli* cultures grow during the antibacterial tests. Neodymium
103 N52 magnets were used as the recollection material. The N52 magnets were purchased from
104 totalElement (totalElement, B1X12X14N52-5PK).

105

106 2.2. AgNPs/Co Synthesis

107 **Figure 2** shows that the synthesis of nanocomposites was carried out in two stages. First,
108 the cobalt cores were synthesized by dissolving ethylene glycol in a precursor solution of cobalt
109 acetate.[25] Hydrazine hydrate was the reducing agent, and PVP was the stabilizing agent. The
110 reaction was carried out in a hot plate with constant stirring at 200 rpm with a stir bar. A solution
111 of 0.4 milliliter (mL) of hydrazine hydrate and 25 mL of ethylene glycol was added dropwise to
112 the 25 mL precursor solution under constant stirring at room temperature. A 50 mL polymer
113 solution was prepared by dissolving PVP into ethylene glycol. This solution was added and stirred
114 for 15 minutes with an overhead stirrer to prevent the cobalt cores adhering to the magnetic stir
115 bar. The solution was heated to 195° C and the temperature was maintained for 30 minutes. 100
116 µg of silver acetate was mixed at 200 rpm for 15 minutes. The solution was then heated to 120° C
117 and kept for 15 minutes under continuous stirring. The finalized nanocomposites were collected

118 with magnets and then washed three times to remove impurities. The AgNPs/Cos were precipitated
119 in an aqueous solution until tested.

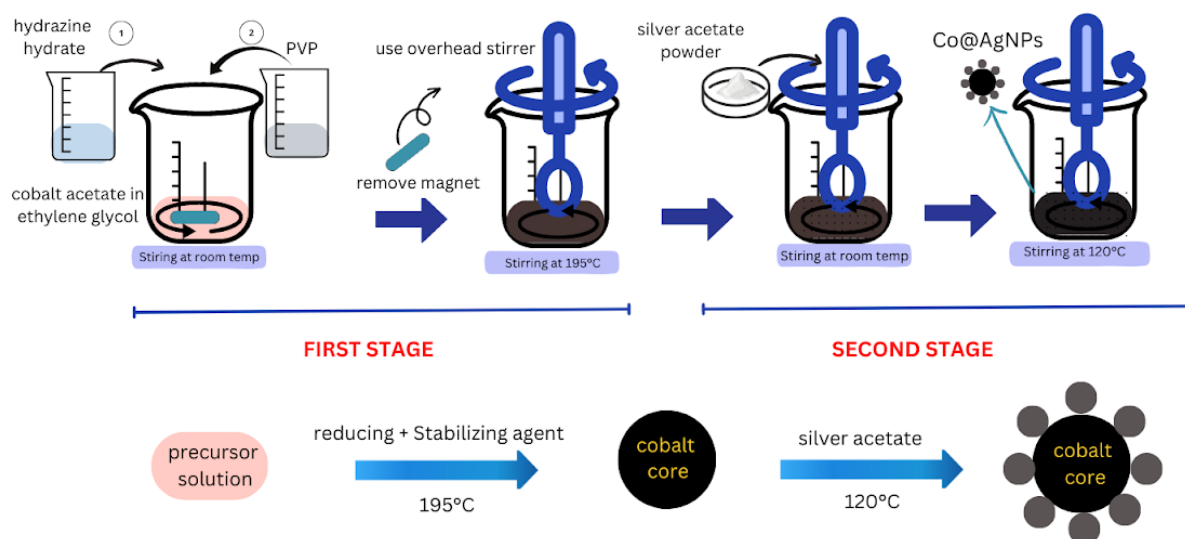


Figure 2. Schematic of Cobalt Core Silver Two-step Process of Nanocomposite Preparation.

120

121 2.3. AgNPs/Co Characterization

122 The AgNPs/Co size was examined with a Phenom Pharos desktop field emission scanning
123 electron microscope (FE-SEM) using a secondary electron detector (SED) from Thermo Scientific
124 (Waltham, MA, USA).

125

126 2.4. Disinfection Tests of *E. coli* Contaminated Water

127 Antibacterial properties were evaluated by the inactivation of bacterial cells on the surface
128 of agar plates via the well diffusion method. To model *E. Coli* contaminated water, *E. coli* dilutions
129 were created by adding 9 mL of distilled (DI) water (Snugell CPAP distilled water) and 1 mL of
130 *E. coli*. Further serial dilutions were carried out until a total dilution factor of 10^{-6} was reached as
131 the synthetic wastewater bacterial concentration.

132 For each experiment, a concentration of 10 mg of AgNPs/Co was used for the antibacterial
133 activity tests. The commercial silver nanoparticle solution was diluted to match this concentration.
134 For comparison, 0.2 mL of the commercial silver nanoparticles were diluted with 0.8 mL of
135 distilled water for a final concentration of 10 mg. 0.25 mL of *E. coli* solution was evenly spread
136 with a cell spreader on the top of nutrient agar plates. The petri dishes were kept in an incubator at
137 37° C for 24 hours.

138 To find the zone of inhibition, an *E. coli* solution of 10^{-3} was spread on the plate.
139 Concentrations of 10,000 µg/mL of both the AgNPs/Co and commercial silver were then added
140 equidistant to each other on the agar plate. The sensitivity of the different concentrations of
141 nanocomposite and the commercial silver nanoparticles to the *E. coli* were determined by the clear
142 zone around the respective samples and the diameters were measured in millimeters (mm).

143 To determine the relationship between reaction time, antibacterial efficiency of AgNPs/Co,
144 and *E. coli* neutralization, further experiments were carried out by manipulating the serial dilutions
145 of the *E. coli* broth. The experiments involve exposing the *E. coli* to four different dilutions of the
146 synthesized nanoparticles for varying time intervals (1, 3, 5, and 10 minutes). The reaction time
147 experiments aimed to identify the optimal duration for the nanoparticles to effectively deactivate
148 the *E. coli*. Additionally, before being dispersed onto nutrient agar-filled plates for further analysis,
149 the *E. coli* suspension is centrifuged for 5 minutes, which helps separate the bacterial cells from
150 the surrounding medium. To ensure the reliability of the results, all tests were conducted in
151 triplicate, meaning each experiment is repeated three times.

152 To evaluate the antibacterial efficiency of AgNPs/Co at various concentrations in
153 neutralizing *E. coli*, the correlation between the concentration of AgNPs/Co, the deactivation of
154 *E. coli*, and the concentration of silver acetate used during the nanocomposite synthesis were

155 investigated. Three different concentrations of the AgNPs/Co (10 mg/mL, 20 mg/mL, 30 mg/mL)
156 and three different concentrations of the silver acetate (50 mg, 100 mg, 200 mg) were tested in
157 triplicate.

158

159 3. RESULTS AND DISCUSSION

160 3.1. AgNPs/Co Characterization

161 By examining the field emission scanning electron microscope (FE-SEM) images (**Figure**
162 **3**), the hypothesis that silver nanoparticles will grow successfully on the surface of cobalt core
163 particles was proven (**Figure 3 (a) and (b)**). SEM micrographs show spherical shape and 3–5 mm
164 size range of nanocomposites. This confirms that the first portion of the two-step process (**Figure**
165 **2**) creates the cobalt core, and the second portion creates the silver nanoparticle decorations.

166

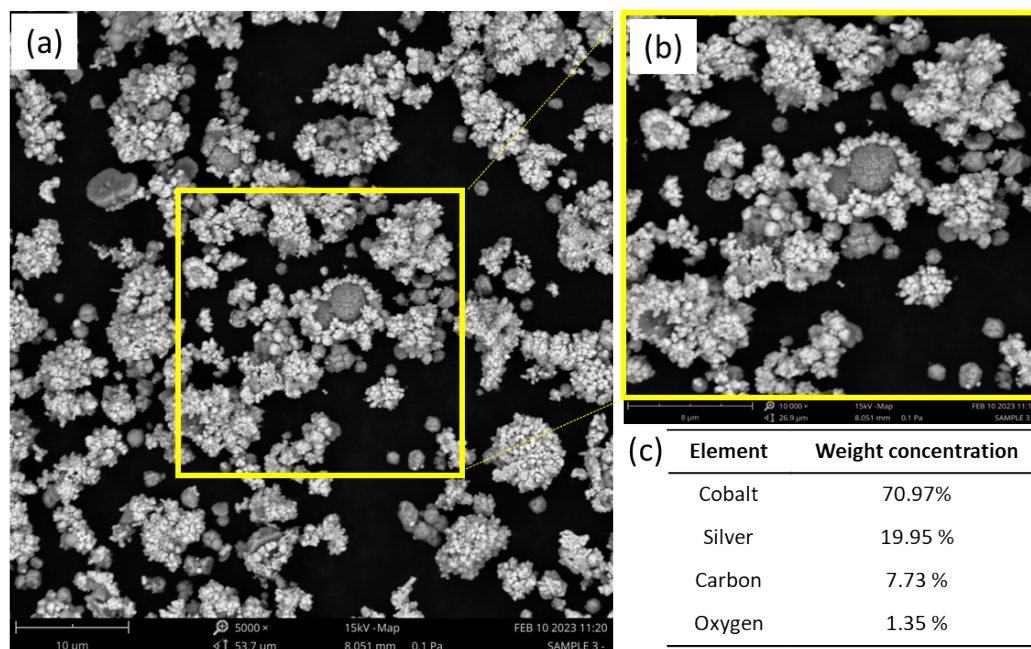


Figure 3. (a, b) Field emission scanning electron microscope (FE-SEM) image of AgNPs/Co nanocomposite synthesized; (c) Energy dispersive spectroscopy (EDS) result of present elements in the nanocomposite sample.

167

168 SEM micrographs showing the spherical morphologies and size range of nanocomposites
169 3-5 μm energy dispersive spectroscopy (EDS) results show that the mixing ratio of silver and
170 cobalt in the synthesized nanocomposite particles is around 2:8 (**Figure 3 (c)**). The silver
171 nanoparticles can also be observed to have a size around 1-2 μm , which is significantly less than
172 the commercial silver nanoparticles, which had a size of around 15 μm . The size of the
173 nanoparticles can be assumed as one of the largest factors in the difference of the efficiency
174 between the AgNPs/Co and the commercial AgNPs.

175 These findings provide strong evidence for the successful growth of silver nanoparticles
176 on the surface of cobalt core particles, resulting in the formation of spherical nanocomposites with
177 a specific size range and a precise mixing ratio of the two components.

178

179 **3.2. Commercial AgNPs versus AgNPs/Co**

180 The disinfection rate of all synthesized AgNPs/Co and commercial AgNPs against tested
181 microorganisms (*E. Coli*) was determined using a diffusion method. **Figure 4** presents images that
182 present the antibacterial activity of 10 mg/mL and 50 mg/mL of the synthesized AgNPs/Co and
183 commercial AgNPs. Both agar plate samples produced a perimeter of bacterial disinfection;
184 however, the AgNPs/Co had a larger perimeter than the commercial AgNPs. The inhibition zones
185 of the AgNPs/Co were 22 mm and 26 mm for the concentrations 10 mg and 50 mg, respectively.

186 The inhibition zones of the commercial AgNPs were 11 mm and 16 mm for the concentrations 10
187 mg and 50 mg, respectively.

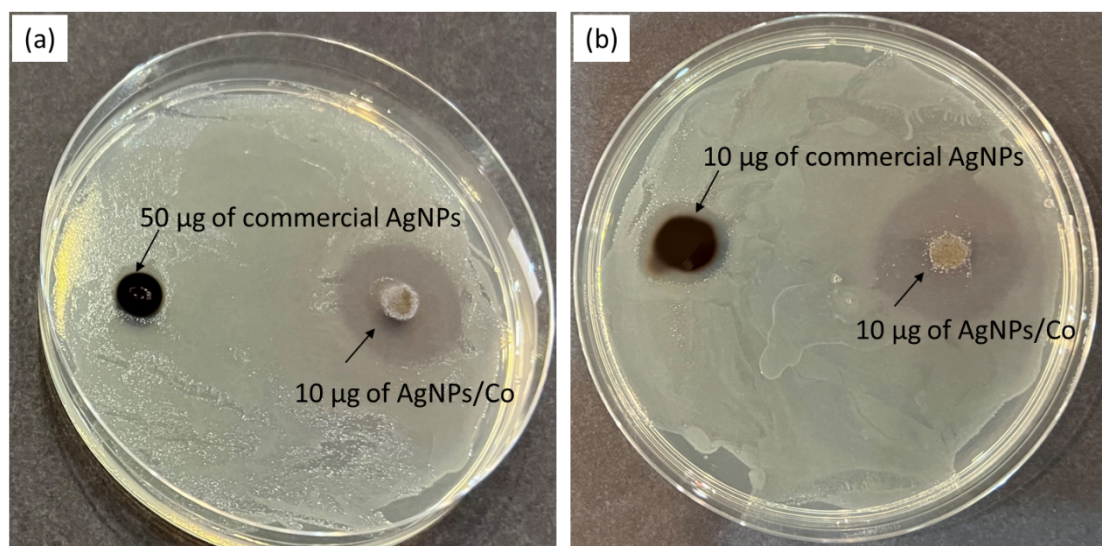


Figure 4. Comparison of the antibacterial efficiency of the commercial silver nanoparticles and cobalt core silver nanoparticles. (a). Side by side comparison of a single dot application of commercial silver nanoparticles (0.05 g/mL) and 1 mL of AgNPs/Co (0.01 g/mL) in an agar plate containing *E. coli*. (b). Side by side comparison of 100 µL of commercial silver nanoparticles (0.01 g/mL) and 1 mL of AgNPs/Co (0.01 g/mL)

188

189 3.3. Magnet Efficiency Test

190 To investigate the magnetism of AgNPs/Co, a comparison was made with commercial
191 silver nanoparticles, both dispersed in water at a concentration of 0.01 gram (g)/mL. **Figure 5**
192 clearly demonstrates that the AgNPs/Co exhibit a reaction to the magnet, whereas the commercial
193 silver nanoparticles do not. Subsequently, a magnet efficiency test was conducted to determine the
194 nanoparticles' removability by magnets. In this test, 0.2 g of the AgNPs/Co were added to 50 mL
195 of water. After stirring the solution for 3 minutes to ensure full suspension of the nanocomposites,
196 a magnet was employed to collect the AgNPs/Co. These nanocomposites were gathered separately

197 and left for 24 hours to dry. Prior to analysis, the weight of the nanoparticles was measured before
198 and after removal from the aqueous suspension to verify their effective extraction by the magnet.
199

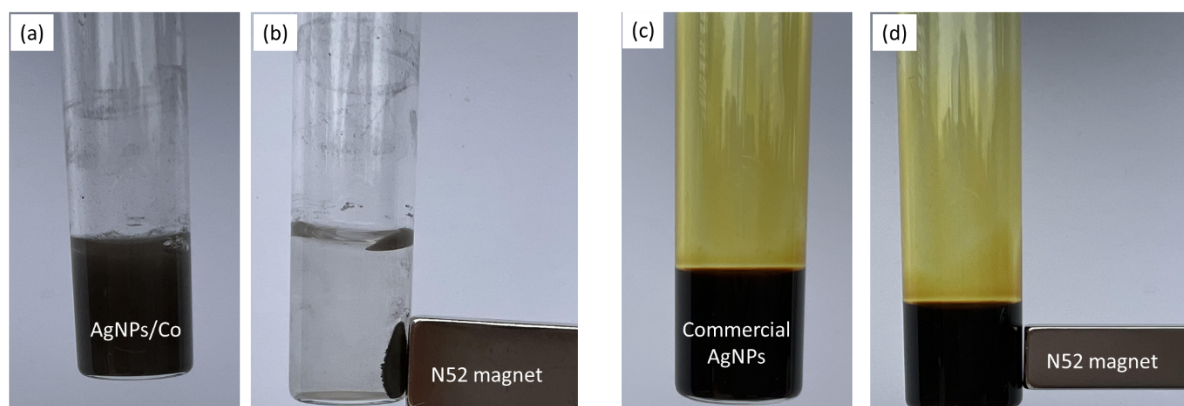


Figure 5. Comparison of Magnetic Response of (a) well dispersed AgNPs/Co (10 µg/mL) in water; (b) reaction of AgNPs/Co (10 µg/mL) to magnet; (c) well dispersed commercial silver nanoparticles (10 µg/mL) in water; (d) no reaction of commercial silver nanoparticles (10 µg/mL) to magnet.

200

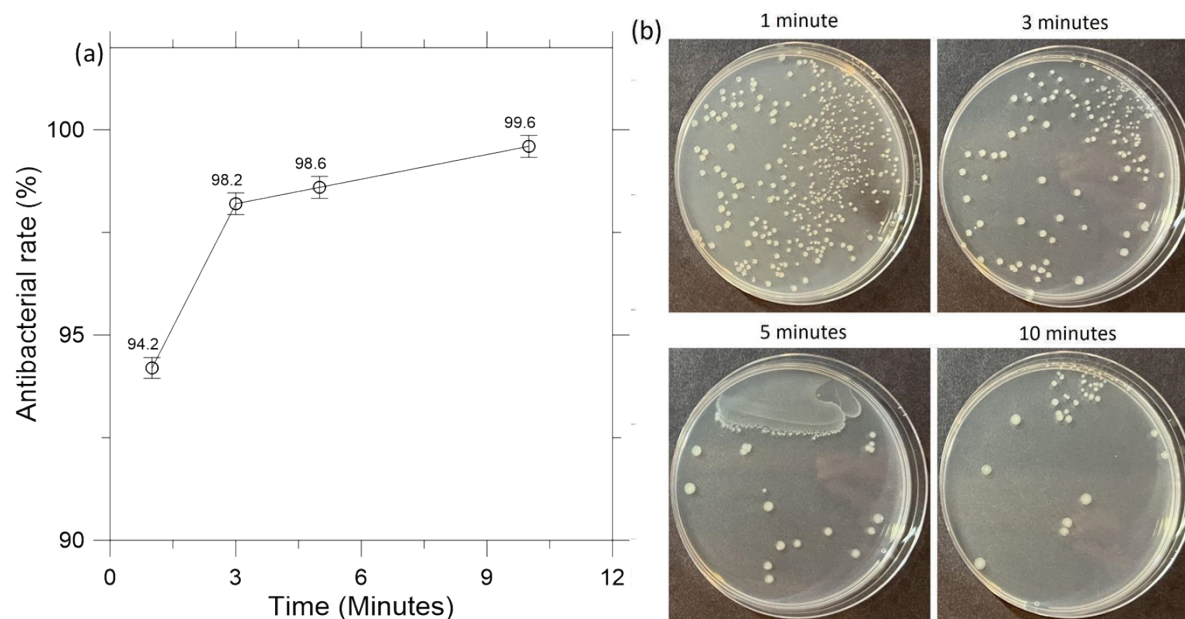
201 After leaving the collected nanocomposites to dry for 24 hours, the weight of the
202 nanocomposites remained at 0.2 g, demonstrating that there is a 100% removal rate of the
203 AgNPs/Co with the N52 magnet. All tests were conducted in triplicate. The AgNPs/Co can be
204 fully collected through magnets, allowing a facile and safe filtration method that prevents the risks
205 of silver poisoning and further environmental and human health damage.

206

207 **3.4. Correlation Between Reaction Time and *E. coli* Cultures**

208 To verify the effectiveness of AgNPs/Co at different concentrations in neutralizing *E. coli*
209 bacteria, the antibacterial rate was calculated by subtracting the total number of colonies from each
210 sample from the total number of colonies from the control, which was then divided by the total
211 number of colonies from the control.

212 The antibacterial results signify a strong correlation between the reaction time of the
213 AgNPs/Co and their antibacterial efficiency (**Figure 6**). The antibacterial rate increases as the
214 reaction time increases. When the AgNPs/Co react with *E. coli* for 1 minute, 94.2% of the bacteria
215 are killed. When the AgNPs/Co react with *E. coli* for 10 minutes, the antibacterial rate increases
216 to 99.6%. The 5.4% augmentation, as illustrated by the graph and images of the plates below,
217 manifests as a noteworthy disparity in both antibacterial efficacy and its potential consequences
218 on human health.



219
220 **Figure 6.** Antibacterial Efficiency of AgNPs/Co (a) *E. coli* antibacterial efficiency rate percentage as a
221 function of time (minutes). (b) Images show the *E. coli* antibacterial efficiency of AgNPs/Co at 1, 3, 5,
222 and 10 minutes.

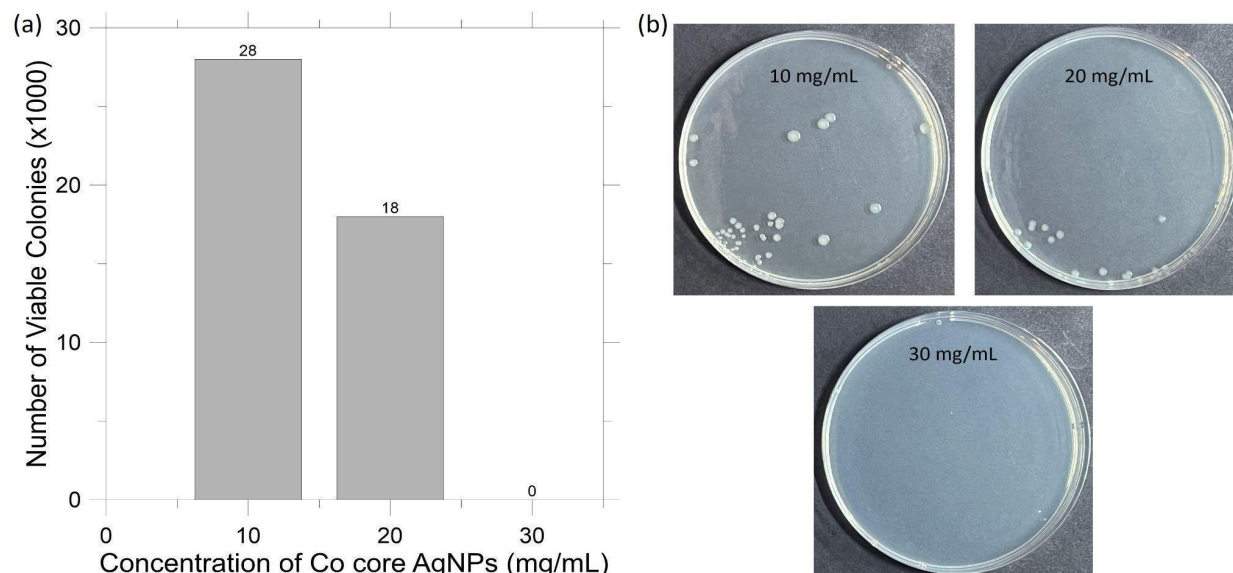
223

224 3.5. Effects of the Material Concentration

225 Concentration was manipulated by decreasing the volume of the solution. The first sample,
226 which had an AgNPs/Co concentration of 10 mg/mL, was created by combining 90 mL of DI water

227 and 10 mL of an *E. coli* solution that was diluted to 10^{-6} . The second sample, with an AgNPs/Co
228 concentration of 20 mg/mL, was created by combining 45 mL of DI water and 5 mL of the same
229 diluted *E. coli* solution. The third sample, with an AgNPs/Co concentration of 30 mg/mL, was
230 created by combining 30 mL of DI water and 3 mL of the same diluted *E. coli* solution.

231 Results show that the concentration of AgNPs/Co plays a strong role in antibacterial
232 efficiency. As the concentration increased, the number of viable *E. coli* colonies decreased. The
233 increased concentration allows the *E. coli* to have increased interactions with the AgNPs/Co. The
234 bacteria's outer membrane interacts with the high surface to volume ratio and small particle size
235 of the AgNPs/Co, which causes a change in the membrane shape and permeability. As the Co-
236 core membranes cross into the *E. coli* cell's membrane, the toxic Co and Ag ions interact with
237 thiol-containing proteins in the cell wall, leading to reactive oxygen species reactions, DNA
238 damage, nucleus breakdown, inhibition of enzyme biosynthesis, and an imbalanced electron
239 transport within the cell.^{21,23} These reactions can result in the *E. coli* cell membrane rupturing
240 and ultimate cell destruction. Therefore, as time increases, based on the concentration of the *E.*
241 *coli* solution, the AgNPs/Co are able to inactivate a larger number of cells, as seen in **Figures 6**
242 **and 7**.

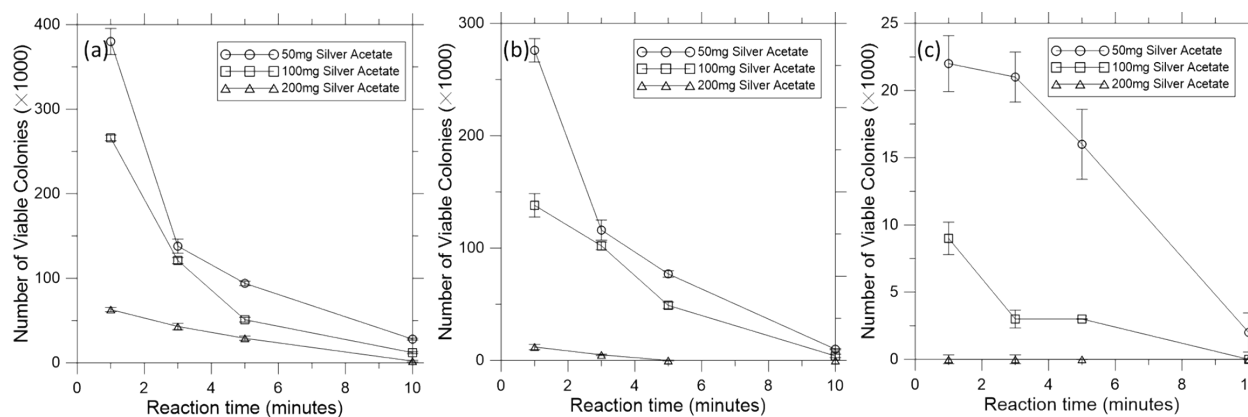


243

244 **Figure 7.** Antibacterial Efficiency of AgNPs/Co in different concentrations; (a) Number of viable
245 colonies with a dilution factor of 10^{-3} with the concentration of AgNPs/Co in mg/mL. (b) Images show
246 the number of viable colonies of AgNPs/Co for each concentration (10 mg/mL, 20 mg/mL, 30 mg/mL).

247

248 Concentrations of the silver acetate were manipulated when synthesizing the AgNPs/Co.
249 Three different concentrations (50 mg, 100 mg, 0.200 mg) were tested for each of the three
250 concentrations of AgNPs/Co. **Figure 8** clearly shows a correlation between the concentration of
251 silver acetate and the antibacterial efficiency of the nanocomposites. With more added silver
252 acetate, more silver nanocomposites would form around the cobalt core, allowing a greater surface
253 area of the silver and a stronger presence of the silver antibacterial properties.



254
255 **Figure 8.** Different concentrations of silver acetate as a synthesis material and reaction time of AgNPs/Co
256 in *E. coli* solution.

257
258 **4. CONCLUSION**

259 The successful synthesis of AgNPs/Co nanocomposites using the polyol process was
260 achieved. The efficiency of these nanocomposites can be adjusted by controlling reaction time and
261 concentration. The study evaluated the magnetic efficiency of the synthesized AgNPs/Co
262 nanocomposite. Subsequently, the disinfection efficiency of AgNPs/Co was assessed in *E. coli*-
263 contaminated water at concentrations ranging from 10 to 50 μg . The results of our research
264 demonstrated an impressive antibacterial efficiency rate of 99.6% when utilizing the proposed
265 AgNPs/Co nanocomposite. Moreover, the novel magnetic nanocomposites exhibited a collecting
266 efficiency rate of 100%, indicating their effectiveness in capturing and removing the AgNPs/Co
267 from the treated water. While further tests regarding the reusability of the nanocomposites were
268 not conducted, it can be inferred that the AgNPs/Co can be reused due to the absence of visible
269 nanoparticle damage, disassociation, or dissolution.

270 The introduction of AgNPs/Co as a disinfection strategy holds great promise for enhancing
271 wastewater treatment processes, ensuring better removal of microbial contaminants, and reducing

272 the release of AgNPs/Co into the environment. Further research and development in this area may
273 lead to the implementation of efficient and sustainable strategies for water disinfection, benefiting
274 both human health and the ecosystem, and contribute to improved wastewater management in
275 healthcare settings.

276 **5. REFERENCES**

- 277 1. Ashbolt NJ. Microbial contamination of drinking water and disease outcomes in developing
278 regions. *Toxicology*. 2004;198: 229–238. doi:10.1016/j.tox.2004.01.030
- 279 2. Chen L, Wang Z. Effects of chlorination, ultraviolet and ozone disinfection on the
280 biotoxicity of triclosan. *Water Supply*. 2018;19: 1175–1180. doi:10.2166/ws.2018.175
- 281 3. Zheng J, Su C, Zhou J, Xu L, Qian Y, Chen H. Effects and mechanisms of ultraviolet,
282 chlorination, and ozone disinfection on antibiotic resistance genes in secondary effluents of
283 municipal wastewater treatment plants. *Chemical Engineering Journal*. 2017;317: 309–316.
284 doi:10.1016/j.cej.2017.02.076
- 285 4. Jung WK, Koo HC, Kim KW, Shin S, Kim SH, Park YH. Antibacterial Activity and
286 Mechanism of Action of the Silver Ion in *Staphylococcus aureus* and *Escherichia coli*.
287 *Applied and Environmental Microbiology*. 2008;74: 2171–2178. doi:10.1128/AEM.02001-
288 07
- 289 5. Yin IX, Zhang J, Zhao IS, Mei ML, Li Q, Chu CH.

The Antibacterial Mechanism of
290 Silver Nanoparticles and Its Application in Dentistry

. *IJN*. 2020;15: 2555–2562.
291 doi:10.2147/IJN.S246764
- 292 6. Morones JR, Elechiguerra JL, Camacho A, Holt K, Kouri JB, Ramírez JT, et al. The
293 bactericidal effect of silver nanoparticles. *Nanotechnology*. 2005;16: 2346.
294 doi:10.1088/0957-4484/16/10/059

- 295 7. Deutscher J, Saier Jr. MH. Ser/Thr/Tyr Protein Phosphorylation in Bacteria – For Long Time
296 Neglected, Now Well Established. *Journal of Molecular Microbiology and Biotechnology*.
297 2006;9: 125–131. doi:10.1159/000089641
- 298 8. Li W-R, Xie X-B, Shi Q-S, Zeng H-Y, OU-Yang Y-S, Chen Y-B. Antibacterial activity and
299 mechanism of silver nanoparticles on *Escherichia coli*. *Appl Microbiol Biotechnol*. 2010;85:
300 1115–1122. doi:10.1007/s00253-009-2159-5
- 301 9. Holt KB, Bard AJ. Interaction of Silver(I) Ions with the Respiratory Chain of *Escherichia*
302 *coli*: An Electrochemical and Scanning Electrochemical Microscopy Study of the
303 Antimicrobial Mechanism of Micromolar Ag⁺. *Biochemistry*. 2005;44: 13214–13223.
304 doi:10.1021/bi0508542
- 305 10. Matés >J. M. Effects of antioxidant enzymes in the molecular control of reactive oxygen
306 species toxicology. *Toxicology*. 2000;153: 83–104. doi:10.1016/S0300-483X(00)00306-1
- 307 11. Marambio-Jones C, Hoek EMV. A review of the antibacterial effects of silver nanomaterials
308 and potential implications for human health and the environment. *J Nanopart Res*. 2010;12:
309 1531–1551. doi:10.1007/s11051-010-9900-y
- 310 12. Deshmukh SP, Patil SM, Mullani SB, Delekar SD. Silver nanoparticles as an effective
311 disinfectant: A review. *Materials Science and Engineering: C*. 2019;97: 954–965.
312 doi:10.1016/j.msec.2018.12.102
- 313 13. De Matteis V. Exposure to Inorganic Nanoparticles: Routes of Entry, Immune Response,
314 Biodistribution and In Vitro/In Vivo Toxicity Evaluation. *Toxics*. 2017;5: 29.
315 doi:10.3390/toxics5040029

- 316 14. Kale SK, Parishwad GV, Patil ASNHAS. Emerging Agriculture Applications of Silver
317 Nanoparticles. *ES Food & Agroforestry*. 2021;Volume 3 (March 2021): 17–22.
- 318 15. Panyala NR, Peña-Méndez EM, Havel J. Silver or silver nanoparticles: a hazardous threat to
319 the environment and human health? *Journal of Applied Biomedicine*. 2008;6: 117–129.
320 doi:10.32725/jab.2008.015
- 321 16. Lu W, Senapati D, Wang S, Tovmachenko O, Singh AK, Yu H, et al. Effect of surface
322 coating on the toxicity of silver nanomaterials on human skin keratinocytes. *Chemical*
323 *Physics Letters*. 2010;487: 92–96. doi:10.1016/j.cplett.2010.01.027
- 324 17. Hadrup N, Sharma AK, Loeschner K. Toxicity of silver ions, metallic silver, and silver
325 nanoparticle materials after in vivo dermal and mucosal surface exposure: A review.
326 *Regulatory Toxicology and Pharmacology*. 2018;98: 257–267.
327 doi:10.1016/j.yrtph.2018.08.007
- 328 18. Levard C, Hotze EM, Lowry GV, Brown GEJr. Environmental Transformations of Silver
329 Nanoparticles: Impact on Stability and Toxicity. *Environ Sci Technol*. 2012;46: 6900–6914.
330 doi:10.1021/es2037405
- 331 19. Ferdous Z, Nemmar A. Health Impact of Silver Nanoparticles: A Review of the
332 Biodistribution and Toxicity Following Various Routes of Exposure. *International Journal of*
333 *Molecular Sciences*. 2020;21: 2375. doi:10.3390/ijms21072375
- 334 20. Grün A-L, Emmerling C. Long-term effects of environmentally relevant concentrations of
335 silver nanoparticles on major soil bacterial phyla of a loamy soil. *Environmental Sciences*
336 *Europe*. 2018;30: 31. doi:10.1186/s12302-018-0160-2

- 337 21. Yu S, Yin Y, Liu J. Silver nanoparticles in the environment. *Environ Sci: Processes Impacts*.
338 2012;15: 78–92. doi:10.1039/C2EM30595J
- 339 22. Fiévet F, Ammar-Merah S, Brayner R, Chau F, Giraud M, Mammeri F, et al. The polyol
340 process: a unique method for easy access to metal nanoparticles with tailored sizes, shapes
341 and compositions. *Chem Soc Rev*. 2018;47: 5187–5233. doi:10.1039/C7CS00777A
- 342 23. Fiorati A, Bellingeri A, Punta C, Corsi I, Venditti I. Silver Nanoparticles for Water Pollution
343 Monitoring and Treatments: Ecosafety Challenge and Cellulose-Based Hybrids Solution.
344 *Polymers*. 2020;12: 1635. doi:10.3390/polym12081635
- 345 24. Kanwal Z, Raza MA, Riaz S, Manzoor S, Tayyeb A, Sajid I, et al. Synthesis and
346 characterization of silver nanoparticle-decorated cobalt nanocomposites (Co@AgNPs) and
347 their density-dependent antibacterial activity. *Royal Society Open Science*. 2019;6: 182135.
348 doi:10.1098/rsos.182135
- 349 25. Ruz P, Sudarsan V. Polyol Method for Synthesis of Nanomaterials. In: Tyagi AK,
350 Ningthoujam RS, editors. *Handbook on Synthesis Strategies for Advanced Materials* :
351 Volume-I: Techniques and Fundamentals. Singapore: Springer; 2021. pp. 293–332.
352 doi:10.1007/978-981-16-1807-9_11
- 353